

# Metal–Organic Framework-Based Antimicrobial Touch Surfaces to Prevent Cross-Contamination

Javier Fonseca, Mary Cano-Sarabia, Pilar Cortés, Jordi Saldo, David Montpeyó, Julia Lorenzo, Montserrat Llagostera, Inhar Imaz,\* and Daniel Maspoch\*

Dedicated to Prof. Omar M. Yaghi on his 60th birth anniversary.

Infection diseases are a major threat to global public health, with nosocomial infections being of particular concern. In this context, antimicrobial coatings emerge as a promising prophylactic strategy to reduce the transmission of pathogens and control infections. Here, antimicrobial door handle covers to prevent cross-contamination are prepared by incorporating iodine-loaded UiO-66 microparticles into a potentially biodegradable polyurethane polymer (Baycusan eco E 1000). These covers incorporate MOF particles that serve as both storage reservoirs and delivery systems for the biocidal iodine. Under realistic touching conditions, the door handle covers completely inhibit the transmission of Gram-positive bacterial species (*Staphylococcus aureus*, and *Enterococcus faecalis*), Gram-negative bacterial species (*Escherichia coli*, *Pseudomonas aeruginosa*, and *Acinetobacter baumannii*), and fungi (*Candida albicans*). The covers remain effective even after undergoing multiple contamination cycles, after being cleaned, and when tinted to improve discretion and usability. Furthermore, as the release of iodine from the door handle covers follow hindered Fickian diffusion, their antimicrobial lifetime is calculated to be as long as approximately two years. Together, these results demonstrate the potential of these antimicrobial door handle covers to prevent cross-contamination, and underline the efficacy of integrating MOFs into innovative technologies.

## 1. Introduction

Infectious diseases are a global public health challenge that causes the loss of 13 million lives annually.<sup>[1]</sup> Over the past 50 years, many new and re-emerging infections have threatened humanity, for example, Legionnaire's disease, Ebola virus, human immunodeficiency viruses, and more recently, SARS-CoV-2, to name a few.<sup>[2]</sup> A particularly concerning category of infectious diseases is nosocomial infections, also known as healthcare-associated infections. They are contracted by patients during their hospital stay for reasons unrelated to their initial illness, causing many deaths every year. In particular, immunosuppressed patients are at a high risk of acquiring opportunistic nosocomial infections. For example, ≈9 to 12% of cancer patients receiving treatment are estimated to develop nosocomial infections.<sup>[3]</sup>

The use of antimicrobial coatings is a promising prophylactic strategy to inhibit

J. Fonseca, M. Cano-Sarabia, I. Imaz, D. Maspoch  
Catalan Institute of Nanoscience and Nanotechnology (ICN2)  
CSIC and The Barcelona Institute of Science and Technology  
Campus UAB, Bellaterra, Barcelona 08193, Spain  
E-mail: inhar.imaz@icn2.cat; daniel.maspoch@icn2.cat

J. Fonseca, M. Cano-Sarabia, D. Maspoch  
Departament de Química  
Facultat de Ciències  
Universitat Autònoma de Barcelona (UAB)  
Cerdanyola del Vallès, Barcelona 08193, Spain

P. Cortés, M. Llagostera  
Departament de Genètica i Microbiologia  
Facultat de Ciències  
Universitat Autònoma de Barcelona (UAB)  
Cerdanyola del Vallès, Barcelona 08193, Spain

 The ORCID identification number(s) for the author(s) of this article can be found under <https://doi.org/10.1002/adma.202403813>

© 2024 The Author(s). Advanced Materials published by Wiley-VCH GmbH. This is an open access article under the terms of the [Creative Commons Attribution-NonCommercial](#) License, which permits use, distribution and reproduction in any medium, provided the original work is properly cited and is not used for commercial purposes.

DOI: 10.1002/adma.202403813

J. Saldo  
Centre d'Innovació  
Recerca i Transferència en Tecnologia dels Aliments (CIRTTA)  
Departament de Ciència Animal i dels Aliments  
Facultat de Veterinària  
Universitat Autònoma de Barcelona (UAB)  
Cerdanyola del Vallès, Barcelona 08193, Spain  
D. Montpeyó, J. Lorenzo  
Institut de Biotecnologia i Biomedicina  
Departament de Bioquímica i de Biologia Molecular  
Universitat Autònoma de Barcelona (UAB)  
Cerdanyola del Vallès, Barcelona 08193, Spain

J. Lorenzo  
Centro de Investigación Biomédica en Red  
Bioingeniería  
Biomateriales y Nanomedicina (CIBER-BBN)  
Cerdanyola del Vallès, Barcelona 08193, Spain  
D. Maspoch  
ICREA  
Pg. Lluís Companys 23, Barcelona 08010, Spain

the attachment and colonization of microorganisms on surfaces and thus reduce the transmission of pathogens and control infections.<sup>[4]</sup> The development of antimicrobial coatings often involves the integration of biocidal agents into polymers or hydrogels, enabling their controlled release over time.<sup>[5]</sup> Biocidal agents commonly incorporated into these coatings consist of antibiotics, quaternary ammonium compounds, chlorhexidine, silver salts, silver nanoparticles, and metal oxide nanoparticles.<sup>[6]</sup> However, these traditional antimicrobial coatings suffer from certain limitations, including microbial resistance, variability in performance depending on surface conditions, and/or low antimicrobial efficacy under real conditions.<sup>[7]</sup> For example, *Enterobacteriaceae* have already shown resistance to silver in silver-based polymeric coatings, probably due to its widespread use in various commercial and medical tools.<sup>[8]</sup> This phenomenon of silver resistance may potentially transfer from the *Enterobacteriaceae* family to other more hazardous families, such as the *Neisseriaceae* or *Staphylococcaceae*. This perspective indeed represents a significant epidemiological concern.

Recently, a new approach for developing antimicrobial coatings has emerged by integrating porous metal–organic frameworks (MOFs)<sup>[9]</sup> within polymers or gels.<sup>[10]</sup> The antimicrobial effect of these coatings can arise from two main strategies. First, they may use the metal centers of the MOFs or release metal ions upon MOF degradation.<sup>[11]</sup> Alternatively, these coatings can efficiently store biocides within the highly porous MOFs and release them gradually over time.<sup>[12]</sup> For example, Dai, Hu, and coworkers have prepared antibacterial wound dressings by integrating MOFs loaded with vancomycin and coated with quaternary ammonium salt chitosan within hydrogels.<sup>[12d]</sup> However, in this latter scenario, the coatings may suffer similar limitations to traditional coatings, as they incorporate similar biocidal agents. In this context, our group has recently shown that iodine, recognized as a highly effective topical antimicrobial agent with a broad spectrum and no reported cases of resistance,<sup>[13]</sup> can be incorporated into iodophilic, porous MOF microparticles; specifically, into microporous pseudo-spherical UiO-66 microparticles.<sup>[14]</sup> In doing so, we have addressed the challenges associated with working with elemental iodine, thereby making its practical application feasible.

Herein, we present the development, prototyping, and fabrication of a MOF-based antimicrobial device: an antimicrobial door handle cover. This innovative cover incorporates MOF particles that serve as both storage reservoirs and delivery systems for the biocidal iodine. To fabricate this prototype, we first optimized the incorporation of spray-dried UiO-66 microparticles, already loaded with iodine, into a non-porous and potentially biodegradable polyurethane polymer known as Baycusan eco E 1000. We chose a polyurethane polymer for its widespread use in fabricating antimicrobial coatings<sup>[15]</sup> and medical devices such as catheters, cardiac pacemaker leads, breast implants, intra-aortic balloons, and gastric balloons.<sup>[16]</sup> Among various polyurethanes, Baycusan eco E 1000 was selected due to its potential biodegradability, non-porosity, waterproof nature, ease of formulation, and derivation from renewable resources, with 50% (w/w) of its composition sourced from carbon renewable resources.<sup>[17]</sup> Once iodine-loaded UiO-66 microparticles were effectively incorporated into this polymer, we proceeded to fabricate the antimicrobial door handle cover devices. These covers release

a small concentration of iodine constantly over time (approximately two years). Testing of this device under conditions simulating real-world door handle touching demonstrated its effectiveness in preventing cross-contamination against Gram-positive and Gram-negative bacteria, as well as fungi. Furthermore, as iodine is stored inside UiO-66 in our device, it helps prevent skin irritation, addressing one of the most common issues associated with the use of iodine as a biocide.

## 2. Results and Discussion

We initiated the synthesis of UiO-66 microparticles using a spray-drying methodology previously reported by our group (Figure 1a,b).<sup>[18]</sup> Powder X-ray diffraction (PXRD) (Figure 1e) and field-emission scanning electron microscopy (FE-SEM) (Figure 1c,d) confirmed the formation of pseudo-spherical crystalline UiO-66 microparticles with diameters ranging from 1 to 4  $\mu\text{m}$ . These microparticles were porous, exhibiting a BET surface area of 965  $\text{m}^2 \text{g}^{-1}$ , as determined by  $\text{N}_2$ -sorption measurements (Figures S1–S3, Supporting Information). Subsequently, iodine was adsorbed onto these UiO-66 microparticles using a solid–gas adsorption setup consisting of two concentric vials: the smaller vial containing the microparticles was enclosed within the larger one containing the iodine, with the larger vial sealed. This setup was placed inside a preheated oven set at 80 °C. At different time intervals, the iodine uptake was determined through weight measurements, resulting in the iodine adsorption isotherm shown in Figure 1f. The isotherm exhibited a rapid increase in iodine adsorption within the initial 12 h, in which intraparticle diffusion was identified as the rate-controlling step. For example, the uptake escalated from 0.08 to 0.33 to 0.71  $\text{mg}_{\text{I}_2} \text{mg}_{\text{UiO-66}}^{-1}$  at 2, 6, and 10 h, respectively. Following this initial step, saturation was nearly achieved at 12 h, with an adsorption of 0.90  $\text{mg}_{\text{I}_2} \text{mg}_{\text{UiO-66}}^{-1}$ . In this second regime, physisorption was found to be the limiting factor in the adsorption of iodine within the UiO-66 microparticles (Figure 1f, Table S1, Supporting Information).

Once the iodine-loaded UiO-66 ( $\text{I}_2@$ UiO-66) microparticles were synthesized, our objective was to prepare antimicrobial films by embedding these  $\text{I}_2@$ UiO-66 microparticles into a polymer, with the ultimate goal of fabricating an antimicrobial door handle cover prototype. For the  $\text{I}_2@$ UiO-66 microparticles, we selected those loaded with iodine for 12 and 6 h, as they demonstrated near-maximum iodine storage (0.90  $\text{mg}_{\text{I}_2} \text{mg}_{\text{UiO-66}}^{-1}$ ) and one-third of the maximum iodine storage capacity (0.33  $\text{mg}_{\text{I}_2} \text{mg}_{\text{UiO-66}}^{-1}$ ), respectively. Both polymeric films were prepared by dispersing 333 mg of each type of microparticles in a 30% (w/w) solution of the polyurethane pre-polymer in water, followed by vigorous stirring at 1500 rpm for 1.5 h. Subsequently, each mixture was uniformly drop-casted onto a glass surface and dried at room temperature for 3 h until the resulting films could be easily detached from the glass slides (Figure 2a). For antimicrobial control experiments, a polyurethane film with UiO-66 microparticles free of iodine was also prepared using the same method.

FE-SEM imaging of the cross-section of the films unveiled a thickness of  $\approx 180 \mu\text{m}$  (Figure 2b; Figure S4, Supporting Information). It also revealed the presence of two distinct regions: a top one, in which the  $\text{I}_2@$ UiO-66 microparticles were uniformly

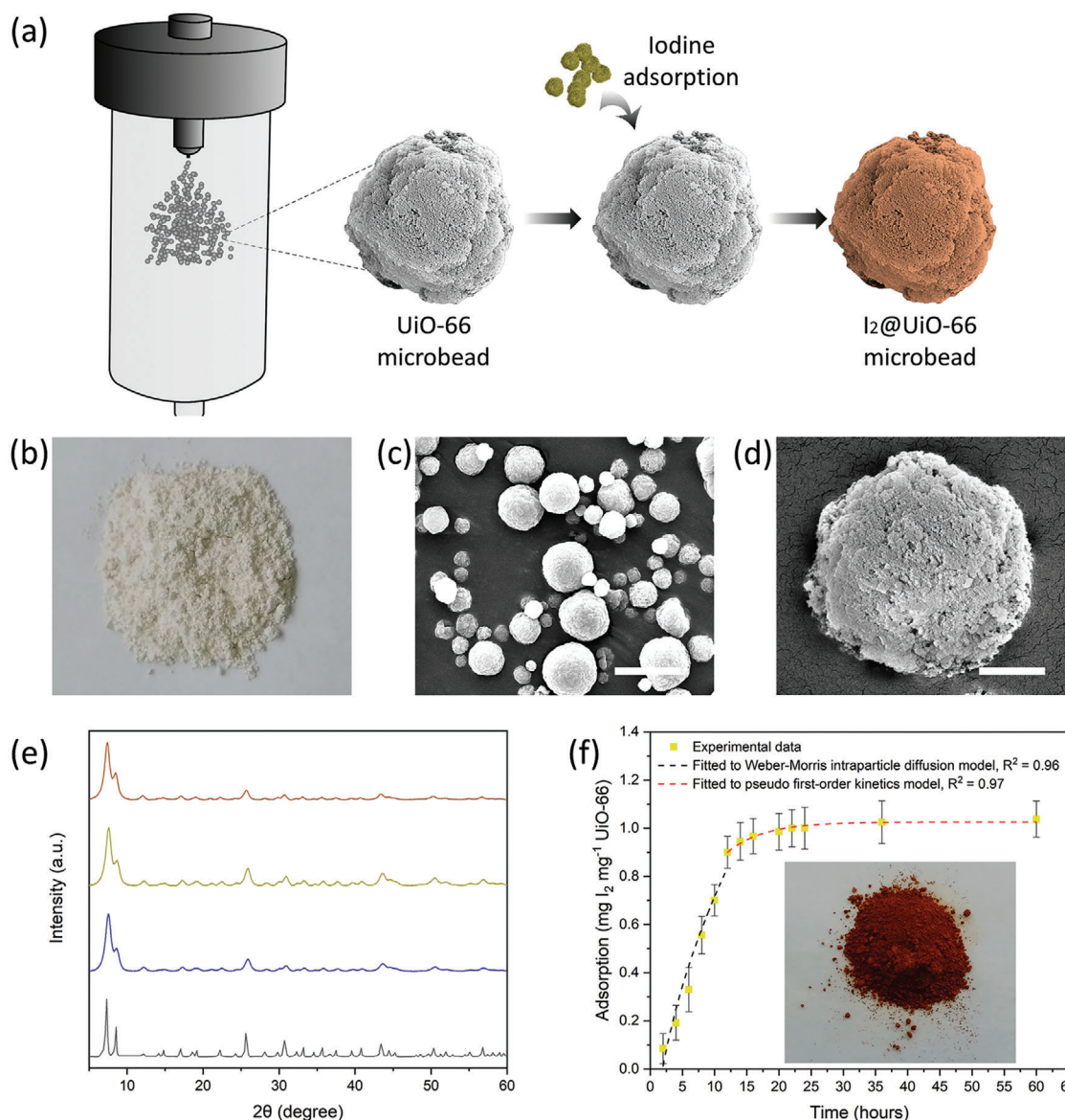


**Figure 1.** a) Schematic illustration of the formation of iodine-loaded UiO-66 microparticles, starting with the spray-drying synthesis of UiO-66 microparticles and concluding with the adsorption of iodine within the microparticles. b) Photograph of the UiO-66 microparticles-based powder. c,d) FE-SEM of UiO-66 microparticles. e) PXRD, arranged from bottom to top, of simulated UiO-66 (black), UiO-66 microparticles (blue), UiO-66 microparticles loaded with iodine for 6 h (yellow), and UiO-66 microparticles loaded with iodine for 12 h (orange). f) Iodine-adsorption isotherm of UiO-66 microparticles at 80 °C. Until 12 h, the data was fitted to the Weber–Morris intraparticle diffusion model; from 12 to 60 h, the data was fitted to the pseudo-first-order kinetic model. Photograph of the UiO-66 microparticles-based powder loaded with iodine for 6 h (inset). Scale bars: 5 μm (c), and 1 μm (d).

dispersed within the polyurethane polymer, and defining the active region of the films (Figure 2c; Figure S4, Supporting Information); and a bottom one, referred to as the polymeric region, in which the I<sub>2</sub>@UiO-66 microparticles were scarce (Figure 2d; Figure S4, Supporting Information). This polymeric region is presumed to provide the necessary characteristics in terms of deformability, fracture toughness, and adhesiveness for utilizing these materials as antimicrobial coatings (see below). Furthermore, PXRD analysis of the coatings indicated that the UiO-66 crystalline structure remained unaltered during the coating formation process (Figure 2e). Thermogravimetric analysis was em-

ployed to estimate the mass percentages of iodine inside the films (Figure S5, Table S2, Supporting Information). The iodine percentages were (w/w)  $5.4 \pm 1.5\%$  ( $0.054 \pm 0.015 \text{ mg}_{\text{I}_2} \text{ mg}_{\text{film}}^{-1}$ ) and  $11.9 \pm 1.8\%$  ( $0.119 \pm 0.018 \text{ mg}_{\text{I}_2} \text{ mg}_{\text{film}}^{-1}$ ) in those films made of I<sub>2</sub>@UiO-66 microparticles loaded with iodine for 6 and 12 h, respectively. These values were slightly lower than the expected 6.2% and 12.8% (w/w) values. We attribute these results to the slight loss of iodine during the film formation process. Finally, N<sub>2</sub>-isotherms performed on the coatings indicated their non-porous nature, suggesting that Baycusan eco E 1000 can effectively function as an enclosure for the I<sub>2</sub>@UiO-66 microparticles.

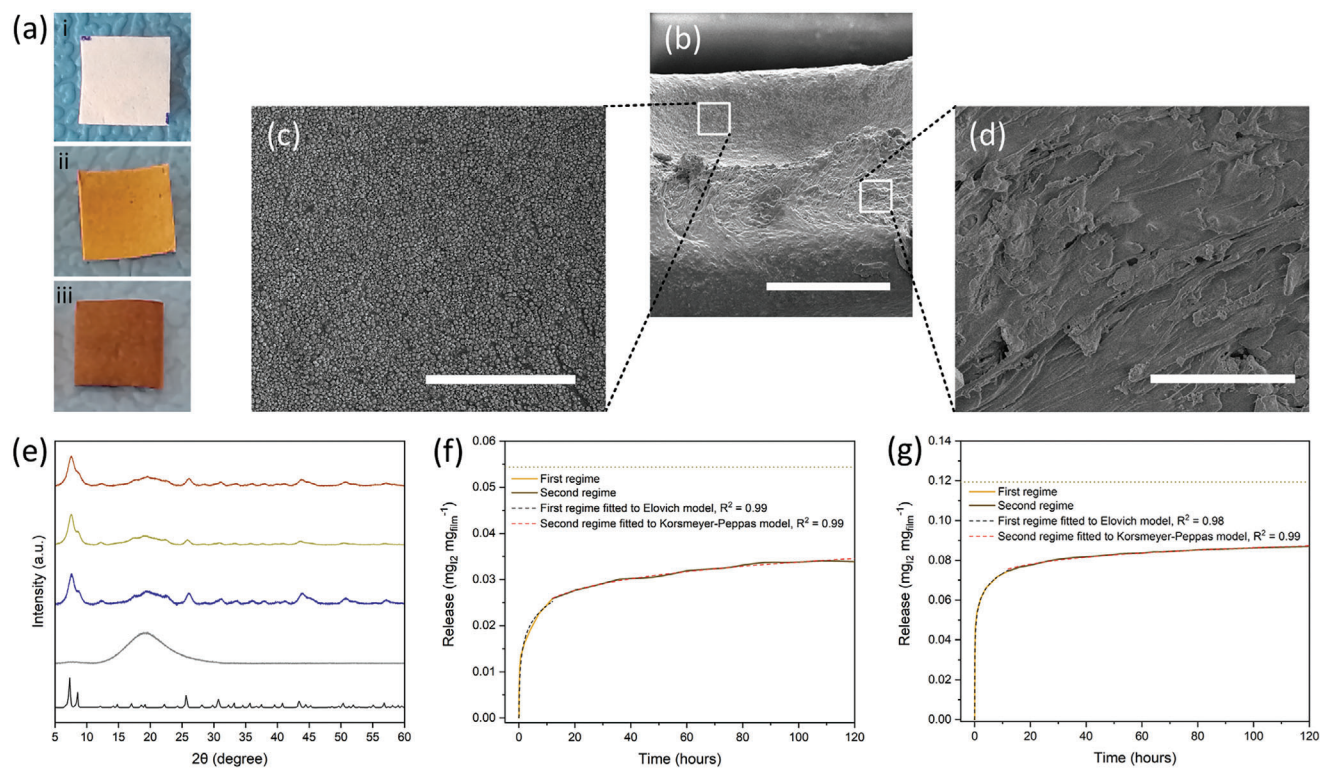


**Figure 2.** a) Photographs of the polyurethane films with UiO-66 microparticles: (i) free of iodine, (ii) loaded with iodine for 6 h, and (iii) loaded with iodine for 12 h. FE-SEM of the cross-section of the films made of  $I_2@UiO-66$  microparticles loaded with iodine for 6 h: b) overall, c) focused on the top area where  $I_2@UiO-66$  microparticles predominate, and d) focused on the bottom area where polyurethane polymer predominates. e) PXRD, arranged from bottom to top, of simulated UiO-66 (black), polyurethane films (grey), and polyurethane films with UiO-66 microparticles free of iodine (blue), loaded with iodine for 6 h (yellow) and loaded with iodine for 12 h (orange). f) Iodine-release profile of polyurethane films containing UiO-66 microparticles loaded with iodine for 6 h, showing the two release regimes, before (orange) and after (dark orange) 12 h. g) Iodine-release profile of polyurethane films containing UiO-66 microparticles loaded with iodine for 12 h, showing the two release regimes, before (orange) and after (dark orange) 12 h. In f,g) the black and red dashed lines represent the Elovich model and the Korsmeier–Peppas model fittings, respectively. The dotted line illustrates iodine initially absorbed into the films that should be completely released over time. Scale bars: 100  $\mu m$  (c), and 10  $\mu m$  (d).

The chemical stability of both types of films was assessed by incubating them in distilled water for 5 days under neutral (pH = 7), acidic (pH = 3), and basic (pH = 10) conditions at 23 and 40 °C. Similarly, the films were evaluated by immersing them in cyclohexane for 5 days at RT and 40 °C. Following incubation, PXRD analysis of the films confirmed their structural integrity, ruling out chemical degradation (Figures S6–S8, Supporting Information). In contrast, when subjected to incubation in polar organic solvents (acetone, dimethylformamide, acetonitrile, or chloroform), the films exhibited partial dissolution within 12 h at both temperatures. We then explored their mechanical properties, focusing on three fundamental aspects: deformability, fracture toughness, and adhesiveness (Table S3, Supporting Information). Low deformability and high fracture toughness are crucial for films as they must resist gripping without deforming or being damaged. Adhesiveness is necessary to ensure the films remain firmly attached. We calculated a deformability modulus of 0.46 N mm<sup>-1</sup> for unloaded polyurethane films and  $\approx 1.17$  N mm<sup>-1</sup> for polyurethane films with  $I_2@UiO-66$  microparticles (Figures S9–S11, Supporting Information). Therefore, the incorporation of microparticles reinforced the polymer, enhancing the rigidity of the films. Likewise, the presence of  $I_2@UiO-66$  microparticles improved

the fracture toughness of the films, with measured values of 0.37 J for polyurethane films and  $\approx 0.55$  J for polyurethane films with iodine-loaded microparticles (Figures S12–S14, Supporting Information). Regarding adhesiveness, the values for polyurethane films and polyurethane films with UiO-66 microparticles loaded for 6 and 12 h were calculated to be 0.005, 0.004, and 0.003 J cm<sup>-2</sup>, respectively (Figures S15–S17, Supporting Information). Therefore, the increased iodine content within the films led to a reduction in film adhesiveness.

Next, we studied the release of iodine from both types of films (Figure 2f,g). To do that, the films were left undisturbed under a continuous nitrogen flow at 30 °C for 5 days immediately after their preparation. Thermogravimetric analysis was then conducted at intervals of 1 s under these conditions. The observed weight losses resulted from the released iodine and the evaporation of the residual water content retained within the films. To account for the contribution of water in the release measurements, we subtracted the weight loss of a film with UiO-66 microparticles free of iodine from the weight losses in iodine-loaded films. Here, the water content within the iodine-loaded films was consistent with that of the unloaded film, as the same initial amount of Baycusan eco E 1000 was used for their formation. Both iodine-loaded films exhibited biphasic iodine

release profiles.<sup>[19]</sup> They showed an initial release phase lasting  $\approx 12$  h, during which iodine was rapidly released. Specifically, a release of  $0.026 \text{ mg}_{\text{I}_2} \text{ mg}_{\text{film}}^{-1}$  (47.4% of the initially stored iodine) and  $0.075 \text{ mg}_{\text{I}_2} \text{ mg}_{\text{film}}^{-1}$  (62.5% of the initially stored iodine) were observed in those films made of  $\text{I}_2@ \text{UiO-66}$  microparticles loaded with iodine for 6 and 12 h, respectively. In this initial phase, the release of iodine from the films was described by the Elovich model, which assumes that the rate of desorption decreases exponentially as the amount of desorbed iodine increases (Figure 2f,g, Tables S4,S5, Supporting Information).<sup>[20]</sup> This initial release phase was succeeded by a phase characterized by a power-law relationship between the cumulative amount of iodine released and the time elapsed within this phase ( $\Delta C \approx (\Delta t)^n$ ). Specifically, the semiempirical Korsmeyer–Peppas model<sup>[21]</sup> was able to describe this iodine release from the coatings:

$$\frac{C_t}{C_\infty} = k \times t^n \quad (1)$$

where  $C_t/C_\infty$  is the fraction of iodine released,  $k$  is a kinetic constant,  $t$  is time, and  $n$  is associated with the mechanism governing the release kinetics. For both films, the value of  $n$  was below 0.45, indicating that iodine release followed hindered Fickian diffusion (Figure 2f,g, Tables S4,S5, Supporting Information).<sup>[21c]</sup> This diffusion regime is characterized by hampered release. According to the semiempirical Korsmeyer–Peppas model, the lifetime of both films was calculated to be 192 and 721 days for those films containing  $\text{I}_2@ \text{UiO-66}$  microparticles loaded for 6 and 12 h, respectively. From this model, we also calculated that iodine would likely be released at a rate of  $10.3 \times 10^{-4} \text{ } \mu\text{g}_{\text{I}_2} \text{ mg}_{\text{film}}^{-1} \text{ min}^{-1}$  ( $\approx 4.8 \times 10^{-3} \text{ } \mu\text{g}_{\text{I}_2} \text{ cm}_{\text{film}}^{-2} \text{ min}^{-1}$ ) and  $4.3 \times 10^{-5} \text{ } \mu\text{g}_{\text{I}_2} \text{ mg}_{\text{film}}^{-1} \text{ min}^{-1}$  ( $\approx 2 \times 10^{-3} \text{ } \mu\text{g}_{\text{I}_2} \text{ cm}_{\text{film}}^{-2} \text{ min}^{-1}$ ) in the films loaded for 6 and 12 h, respectively. These results confirmed that the polyurethane polymer properly encloses the  $\text{I}_2@ \text{UiO-66}$  microparticles, allowing a slow and continuous iodine release.

Once the films containing the  $\text{I}_2@ \text{UiO-66}$  microparticles were synthesized, we proceeded to fabricate two prototypes of door handle covers using both types of films. Initially, we crafted films with dimensions of 50 cm in width and 10 cm in height, precisely tailored to match the length of the door handle serving as a template (10 cm). These films were then tinted with blue acrylic paint to conceal their inherent yellow color, commonly associated with urgent attention in healthcare facilities, thus enhancing their aesthetic appeal. Subsequently, the resulting films were affixed onto the surface of the door handle template through their polymeric region, exposing their active region to the air. The films were wound around the cylindrical door handle template up to 8 times, ensuring uniformity in the final covers (Figure 3a; Figure S18, Supporting Information). It is worth noting that, to maintain adhesiveness, the films were applied to the door handle surface immediately after detachment from the glass surface where they were synthesized. When desired, the resulting door handle covers could be removed from their template by carefully twisting them with sufficient force to detach. Consequently, these covers could then be affixed to other door handles (Figure 3b).

After fabricating the door handle covers, our next step was to ensure they did not present risks associated with excessive iodine exposure, particularly concerning skin irritation. To do

that, we conducted an in vitro evaluation of the cytotoxicity of both door handle cover prototypes using HaCaT cells, which are human keratinocytes representative of human skin cells.<sup>[22]</sup> Our covers demonstrated minimal cytotoxicity, with  $\text{IC}_{50}$  values against HaCaT cells ranging from 0.191 to  $0.457 \text{ mg}_{\text{I}_2} \text{ cm}_{\text{film}}^{-2}$ , with 95% confidence intervals. Furthermore, we provided an interpretation of these results in terms of practical implications. Considering the release rates of iodine from the covers, we estimated the time required for the covers to inhibit 50% of HaCaT cells if in contact with the skin. These estimates indicate that the covers would need to be in contact with the skin for an extended period, far beyond typical durations, to exert cytotoxic effects. In numbers, considering the release rate of iodine from the cover containing  $\text{I}_2@ \text{UiO-66}$  microparticles loaded for 6 h was  $\approx 4.8 \times 10^{-3} \text{ } \mu\text{g}_{\text{I}_2} \text{ cm}_{\text{film}}^{-2} \text{ min}^{-1}$ , the cover would inhibit 50% of HaCaT cells if in contact with the skin for  $\approx 28$  days. This time is even longer ( $\approx 158$  days) if one considers the results obtained for the cover containing  $\text{I}_2@ \text{UiO-66}$  microparticles loaded for 12 h. Given that these covers are unlikely to be in contact with the skin for more than a few minutes, the results showed no significant effects on cell viability with either cover, indicating they were non-cytotoxic upon release and unlikely to induce skin irritation (Figure S19, Table S6, Supporting Information).

Having confirmed that our door handle cover prototypes are not skin irritants, we proceeded to assess their antimicrobial activity to prevent cross-contamination of pathogens by hand. For this, we followed a methodology based on using RODAC plates to evaluate the contact-mediated microbial transference on surfaces, similar to the standardized protocol ASTM E3285-22 or that used in other studies.<sup>[23]</sup> This protocol aimed to simulate the contamination of a door handle and then, the potential transmission of the microorganisms by a hand that touches the same door handle (Figure 3c). We started by slicing  $1 \times 1 \text{ cm}^2$  pieces of the door handle covers. These pieces were then contaminated by dropping  $10 \text{ } \mu\text{l}$  of a microbial suspension in PBS 1X (microbial concentration of  $10^5 \text{ CFU mL}^{-1}$ ) on them, resulting in  $10^3 \text{ CFU film}^{-1}$ . Then, the pieces were incubated at room temperature for 1, 2, and 5 min. After incubation, to simulate the cross-contamination by a hand that touches the door handle cover, tryptone soya agar (TSA) RODAC plates were put in contact with the contaminated pieces for 5–6 s. Uniform and similar pressure (“touching pressure”) was applied in all experiments. The RODAC plates were incubated at  $37 \text{ }^\circ\text{C}$  for 18 h. Finally, for each experiment, the number of colonies (expressed as colony forming units, CFUs) on the RODAC plate was counted to evaluate the antimicrobial performance of the door handle cover prototypes to prevent cross-contamination. As a control, we repeated all experiments using a door handle cover with UiO-66 microparticles not loaded with iodine and compared these results with the corresponding ones loaded with iodine. Also, very important to consider is that the evaluation of the antimicrobial activity of the door handle covers was performed out of the iodine burst release regime. To this end, once the door handle covers were fabricated, they were exposed to the air at room temperature for a minimum of 12 h. This decision was taken to avoid unreproducible conditions and evaluate the more constant, slower, and long-lasting iodine release regime (rate =  $\approx 4.8 \times 10^{-3} \text{ } \mu\text{g}_{\text{I}_2} \text{ cm}_{\text{film}}^{-2} \text{ min}^{-1}$  or  $\approx 2.0 \times 10^{-3} \text{ } \mu\text{g}_{\text{I}_2} \text{ cm}_{\text{film}}^{-2} \text{ min}^{-1}$ ) of the door handle covers, better approaching to real user conditions. Moreover, the door handle

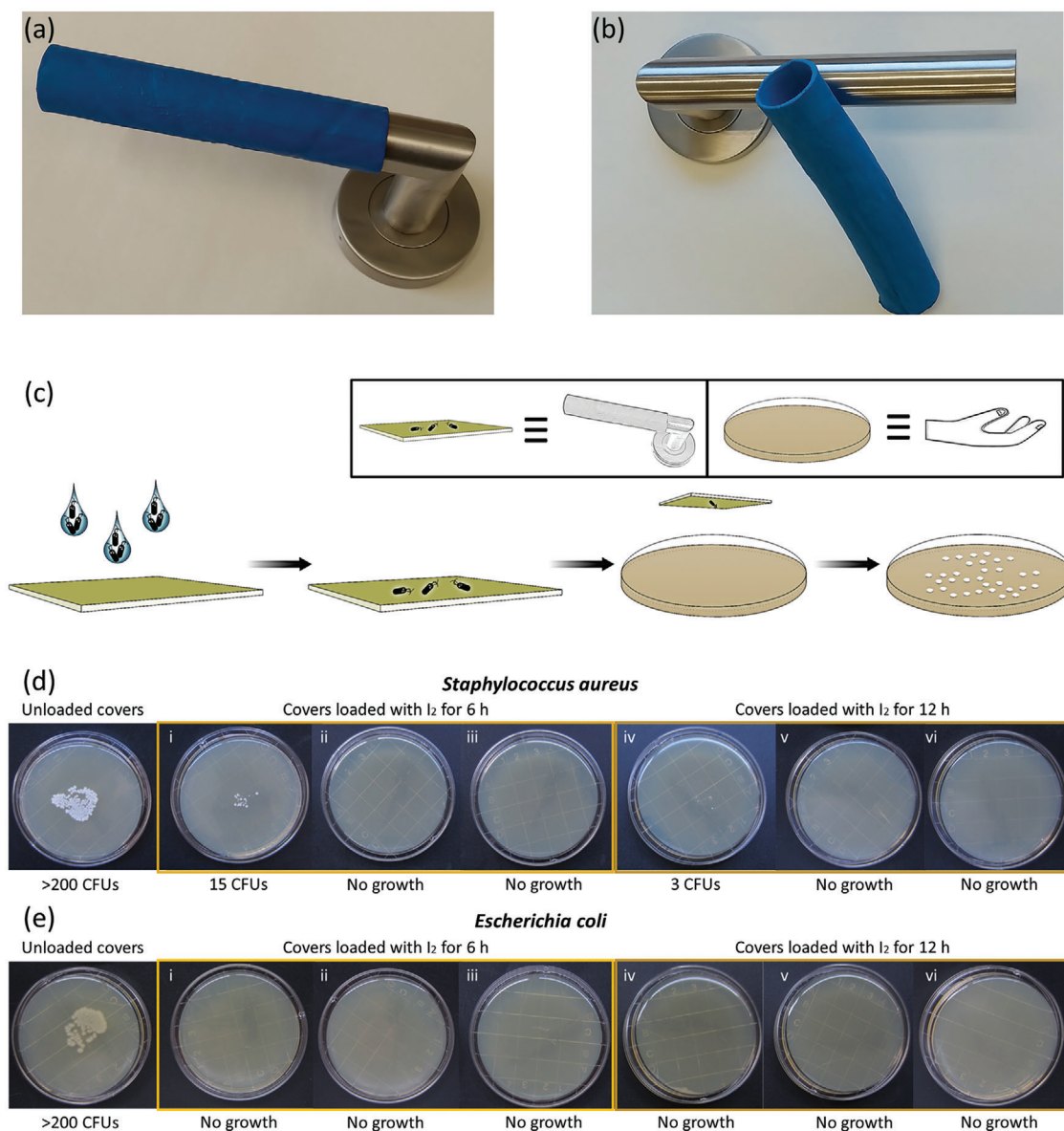


**Figure 3.** a, b) Photograph of the door handle cover made of polyurethane film with UiO-66 microparticles loaded with iodine for 6 h. c) Schematic illustration of the protocol performed to validate the antimicrobial activity of the door handle cover prototypes. Growth-inhibition in d) *S. aureus* produced by the door handle cover loaded with iodine for 6 h when incubated with the microbial suspensions for (i) 1, (ii) 2, and (iii) 5 min; and by the door handle cover loaded with iodine for 12 h when incubated with the microbial suspensions for (iv) 1, (v) 2, and (vi) 5 min. Growth-inhibition in e) *E. coli* produced by the door handle cover loaded with iodine for 6 h when incubated with the microbial suspensions for (i) 1, (ii) 2, and (iii) 5 min; and by the door handle cover loaded with iodine for 12 h when incubated with the microbial suspensions for (iv) 1, (v) 2, and (vi) 5 min. Left: photographs of TSA RODAC plates that were in contact with iodine-unloaded covers previously incubated with the corresponding pathogens. Right: photographs of TSA RODAC plates that were in contact with the covers previously incubated with the corresponding pathogens.

covers were tested prior to coloring them with blue acrylic paint to prevent any traces of blue ink on the RODAC plates, ensuring clarity during colony counting.

The initial antibacterial activity assessments of both door handle cover prototypes targeted the representative Gram-positive bacterium *Staphylococcus aureus*, a significant human pathogen associated with nosocomial pneumonia,<sup>[24]</sup> and the representative Gram-negative bacterium *Escherichia coli*, known as a common cause of nosocomial urinary tract infection.<sup>[25]</sup> Both proto-

types reduced the bacterial growth of *S. aureus*, even after just 1 min of incubation, and completely inhibited it after 2 and 5 min (Figure 3d). Specifically, when incubating the door handle prototypes for 1 min with this Gram-positive bacterium, we observed 15 and 3 CFUs for those prototypes loaded with iodine for 6 and 12 h, respectively. When assessing the activity against *E. coli*, both prototypes were found to completely inhibit bacterial growth after 1, 2, and 5 min of incubation (Figure 3e). Interestingly, identical results using an incubation time of 2 min were obtained when

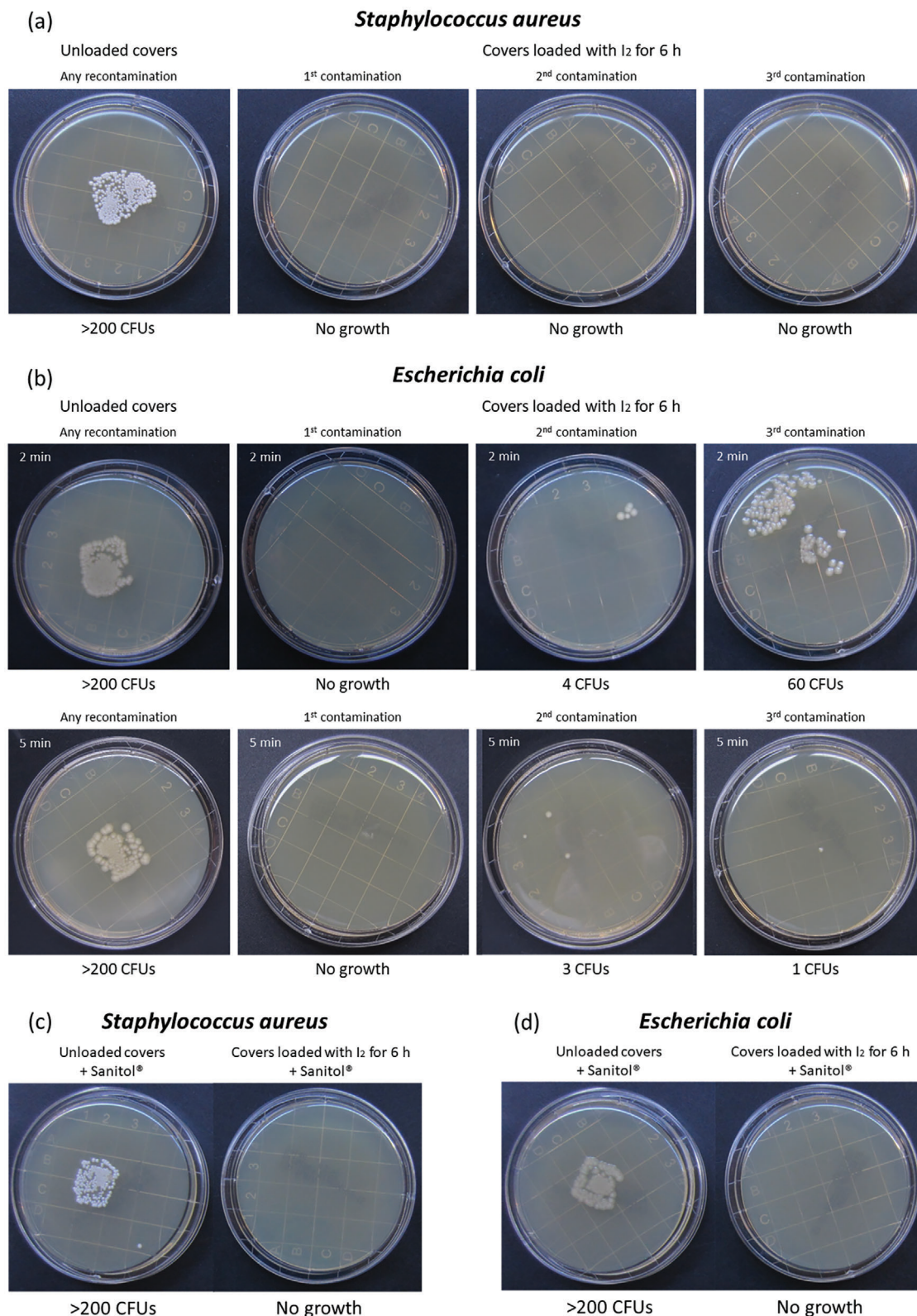


**Figure 4.** Growth-inhibition in a) *S. aureus* produced by the door handle cover after various cycles of contamination using 2 min of incubation. Growth-inhibition in b) *E. coli* produced by the door handle cover after various cycles of contamination using 2 or 5 min of incubation. Growth inhibition in c) *S. aureus* and d) *E. coli* produced by the door-handle cover after subjecting it to a commercial disinfectant (Sanitol). Left: photographs of TSA RODAC plates that were in contact with iodine-unloaded covers previously incubated with the corresponding pathogens. Right: photographs of TSA RODAC plates that were in contact with the covers previously incubated with the corresponding pathogens.

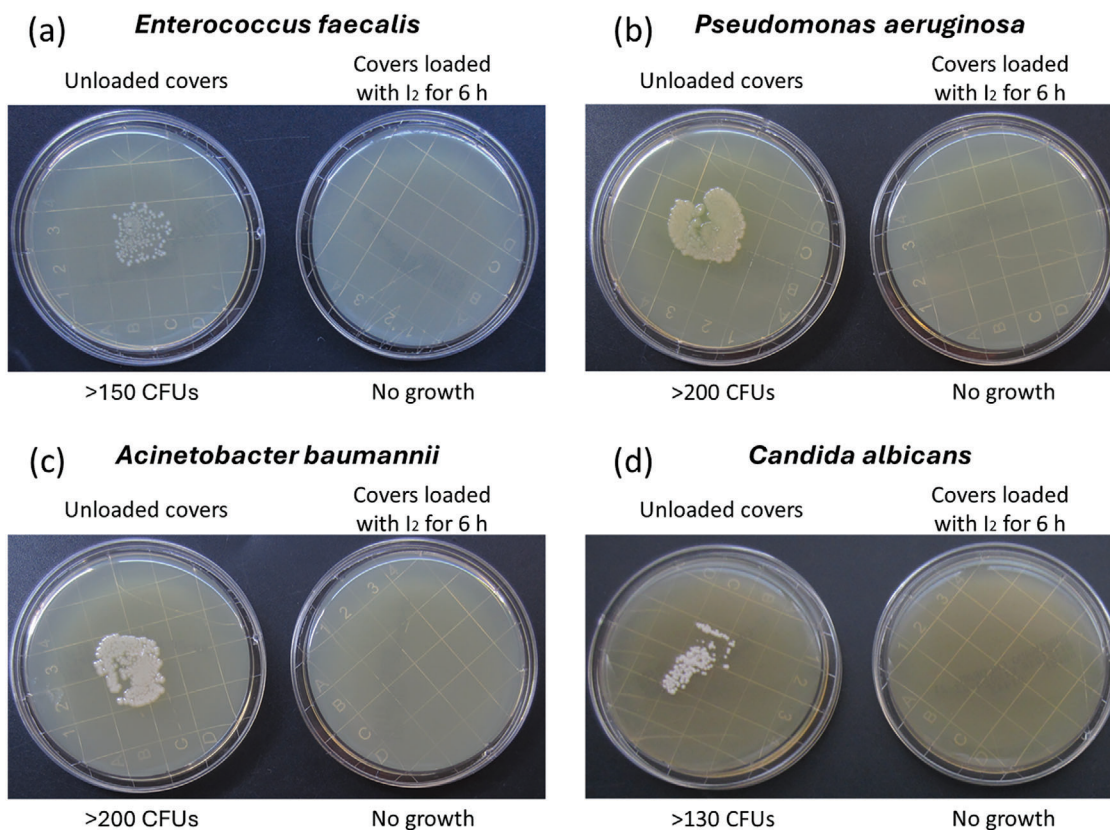


**Figure 5.** Growth-inhibition in a) *E. faecalis*, b) *P. aeruginosa*, c) *A. baumannii*, and d) *C. albicans* produced by the door handle cover using 2 min of incubation time. Left: photographs of TSA RODAC plates that were in contact with iodine-unloaded covers previously incubated with the corresponding pathogens. Right: photographs of TSA RODAC plates that were in contact with the covers previously incubated with the corresponding pathogens. Sabouraud RODAC agar plates were used for selective growth and enumeration of *C. albicans* instead of TSA RODAC plates.

a door handle cover was kept under air for 5 days after its fabrication, which is consistent with the long-lasting release of iodine facilitated by hindered Fickian diffusion (Figure S20, Supporting Information). Contrariwise, control experiments performed on the door handle covers not loaded with iodine showed that they cannot prevent cross-contamination. Indeed, significant bacterial growth (>200 CFU) was always found for both bacteria and different incubation times.

Given all the results outlined above, in which both prototypes show almost identical antimicrobial activity against bacterial cross-contamination, we decided to continue this evaluation study only with the door handle prototype loaded with iodine for 6 h. By doing so, we assumed that if this prototype shows activity in inhibiting pathogen growth, its counterpart, the door handle cover loaded with iodine for 12 h, would likely demonstrate similar or potentially superior performance. Using this selected prototype, we then performed an experiment simulating the effect of touching the door handle for a total of three times with a hand. For this, we consecutively repeated the protocol described above (using an incubation time of 2 min) twice, and three times on the same piece of door handle cover. Remarkably, we found that our door handle prototype was able to prevent the consecutive cross-contamination of *S. aureus*, completely inhibiting their growth and transmission (Figure 4a). Contrariwise, the number of *E. coli* colonies was found to increase from 0 CFUs to 4 to 60 CFUs after

the first, second, and third recontamination, respectively. However, inhibition of *E. coli* growth and transmission was achieved increasing the incubation time of 5 min (Figure 4b).

To extend the evaluation of the antimicrobial performance to other bacteria, we also tested the efficacy of our door handle cover against *Enterococcus faecalis*, a Gram-positive bacterium commonly associated with nosocomial urinary tract infections, bacteremia, and infective endocarditis;<sup>[26]</sup> *Pseudomonas aeruginosa*, a Gram-negative bacterium that is an important pathogen of nosocomial lower respiratory tract infection especially in intensive care units,<sup>[27]</sup> and *Acinetobacter baumannii*, a Gram-negative bacterium that is a nosocomial pathogen that causes bloodstream infections in critically ill patients.<sup>[28]</sup> Again, for all these bacteria, complete growth inhibition was observed after 1, 2, and 5 min of incubation (Figure 5a–c; Figures S21–S23, Supporting Information). Also, we proceeded to assess our door handle cover against other types of pathogens such as the yeast *Candida albicans*, which is a common cause of nosocomial mucosal infections (e.g., invasive candidiasis).<sup>[29]</sup> Similar to the bacteria, we found complete inhibition of this fungus after 1, 2, and 5 min of incubation (Figure 5d; Figure S24, Supporting Information).

Having demonstrated the efficacy to prevent cross-contamination by hand, we also tested the effect of incorporating a dye like blue acrylic paint in the door handle cover. This modification served to mask the inherent yellow color of the

cover coming from the iodine. The activity of the colored door handle cover was assessed against both *S. aureus* and *E. coli* after a 2 min incubation (Figure S25, Supporting Information), confirming that this dye does not compromise the antimicrobial activity of the prototype. Finally, an important consideration when utilizing these door handle covers in real conditions (e.g., healthcare facilities) is that these surfaces are routinely cleaned with disinfectants. For this reason, we explored the activity of the prototype after subjecting it to five passages of a swab moistened with a commercial disinfectant (Sanitol), showing that it still inhibits the growth of both *S. aureus* and *E. coli* after 2 min of incubation (Figure 4c,d).

### 3. Conclusion

In conclusion, we have demonstrated the utilization of MOFs in the development and fabrication of prototypes for antimicrobial door handle covers. These covers efficiently prevent cross-contamination against Gram-positive and Gram-negative bacterial species, as well as fungi. This preventive effect was sustained over three contamination cycles, even after the door handle cover was cleaned with a disinfectant or tinted to enhance discretion and usability. Collectively, these results highlight the potential of these antimicrobial door handle covers to significantly reduce the transmission of pathogens and control infections. Furthermore, it underscores the efficacy of integrating MOFs into innovative technologies.

### Supporting Information

Supporting Information is available from the Wiley Online Library or from the author.

### Acknowledgements

This work was funded by the European Research Council Executive Agency under the powers delegated by the European Commission, Project 101062041 – SAFE-ON, the Catalan AGAUR (project 2017 SGR 238), the MCIN/AEI/10.13039/501100011033 (project PID2021-127983OB-C22), and the CERCA Program/Generalitat de Catalunya. ICN2 was supported by the Severo Ochoa program from the Spanish MINECO (grant CEX2021-001214-S).

### Conflict of Interest

The authors declare no conflict of interest.

### Data Availability Statement

The data that support the findings of this study are available from the corresponding author upon reasonable request.

### Keywords

antimicrobial coatings, delivery systems, iodine, metal–organic frameworks (MOFs), prototypes

Received: March 14, 2024

Revised: April 30, 2024

Published online:

- [1] M. L. Cohen, *Nature* **2000**, 406, 762.
- [2] a) B. A. Cunha, A. Burillo, E. Bouza, *Lancet* **2016**, 387, 376; b) S. T. Jacob, I. Crozier, W. A. Fischer II, A. Hewlett, C. S. Kraft, M.-A. de La Vega, M. J. Soka, V. Wahl, A. Griffiths, L. Bollinger, J. H. Kuhn, *Nat. Rev. Dis. Primers* **2020**, 6, 13; c) J. O. Kahn, B. D. Walker, *N. Engl. J. Med.* **1998**, 339, 33; d) J. D. Sachs, S. S. A. Karim, L. Akin, J. Allen, K. Brosbøl, F. Colombo, G. Cuevas Barron, M. F. Espinosa, V. Gaspar, A. Gavia, A. Haines, P. J. Hotez, P. Koundouri, F. Larrain Bascuñán, J.-K. Lee, M. A. Pate, G. Ramos, K. S. Reddy, I. Serageldin, J. Thwaites, V. Vike-Freiberga, C. Wang, M. K. Were, L. Xue, C. Bahadur, M. E. Bottazzi, C. Bullen, G. Laryea-Adjei, Y. B. Amor, O. Karadag, et al., *Lancet* **2022**, 400, 1224.
- [3] M. Kamboj, K. A. Sepkowitz, *Lancet Oncol.* **2009**, 10, 589.
- [4] K. Glinel, P. Thebault, V. Humblot, C. M. Pradier, T. Jouenne, *Acta Biomater.* **2012**, 8, 1670.
- [5] L. Liu, H. Shi, H. Yu, S. Yan, S. Luan, *Biomater. Sci.* **2020**, 8, 4095.
- [6] a) B. Wang, H. Liu, Z. Wang, S. Shi, K. Nan, Q. Xu, Z. Ye, H. Chen, *J. Mater. Chem. B* **2017**, 5, 1498; b) D. Druvari, N. D. Koromilas, V. Bekiari, G. Bokias, J. K. Kallitsis, *Coatings* **2018**, 8, 8; c) R. Ben-Knaz, R. Pedahzur, D. Avnir, *Adv. Funct. Mater.* **2010**, 20, 2324; d) W. Sim, R. T. Barnard, M. A. T. Blaskovich, Z. M. Ziora, *Antibiotics* **2018**, 7, 93; e) I. I. Niyonshuti, V. R. Krishnamurthi, D. Okyere, L. Song, M. Benamara, X. Tong, Y. Wang, J. Chen, *ACS Appl. Mater. Interfaces* **2020**, 12, 40067; f) U. Kadiyala, N. A. Kotov, J. S. VanEpps, *Curr. Pharm. Des.* **2018**, 24, 896.
- [7] M. Cloutier, D. Mantovani, F. Rosei, *Trends Biotechnol.* **2015**, 33, 11.
- [8] L. Rizzello, P. P. Pompa, *Chem. Soc. Rev.* **2014**, 43, 1501.
- [9] a) O. M. Yaghi, M. O'Keeffe, N. W. Ockwig, H. K. Chae, M. Eddaoudi, J. Kim, *Nature* **2003**, 423, 705; b) H. Furukawa, K. E. Cordova, M. O'Keeffe, O. M. Yaghi, *Science* **2013**, 341, 1230444; c) O. K. Farha, J. T. Hupp, *Acc. Chem. Res.* **2010**, 43, 1166; d) H.-C. Zhou, S. Kitagawa, *Chem. Soc. Rev.* **2014**, 43, 5415; e) Z. Chen, K. O. Kirlikovali, L. Shi, O. K. Farha, *Mater. Horiz.* **2023**, 10, 3257; f) R. Freund, O. Zaremba, G. Arnauts, R. Ameloot, G. Skorupskii, M. Dincă, A. Bavykina, J. Gascon, A. Ejsmont, J. Goscińska, M. Kalmutzki, U. Lächelt, E. Ploetz, C. S. Diercks, S. Wuttke, *Angew. Chem.* **2021**, 60, 23975.
- [10] a) A. K. Bindra, D. Wang, Y. Zhao, *Adv. Mater.* **2023**, 35, 2300700; b) R. Li, T. Chen, X. Pan, *ACS Nano* **2021**, 15, 3808; c) R. Riccò, W. Liang, S. Li, J. J. Gassensmith, F. Caruso, C. Doonan, P. Falcaro, *ACS Nano* **2018**, 12, 13; d) W. Liang, P. Wied, F. Carraro, C. J. Sumby, B. Nidetzky, C.-K. Tsung, P. Falcaro, C. J. Doonan, *Chem. Rev.* **2021**, 121, 1077; e) P. Escamilla, L. Bartella, S. Sanz-Navarro, R. M. Percoco, L. Di Donna, M. Prejanò, T. Marino, J. Ferrando-Soria, D. Armentano, A. Leyva-Pérez, E. Pardo, *Chem. - Eur. J.* **2023**, 29, 202301325; f) C. Pettinari, R. Pettinari, C. Di Nicola, A. Tombesi, S. Scuri, F. Marchetti, *ACS Appl. Mater. Interfaces* **2017**, 9, 4440; g) Z. Chen, F. Xing, P. Yu, Y. Zhou, R. Luo, M. Liu, U. Ritz, *Acta Biomater.* **2024**, 175, 27.
- [11] a) Z. Liu, J. Ye, A. Rauf, S. Zhang, G. Wang, S. Shi, G. Ning, *Biomater. Sci.* **2021**, 9, 3851; b) X. Fan, F. Yang, J. Huang, C. N. Y. Yang, W. Zhao, C. Cheng, C. Zhao, R. Haag, *Nano Lett.* **2019**, 19, 5885; c) Y. Yang, Y. Deng, J. Huang, X. Fan, C. Cheng, C. Nie, L. Ma, W. Zhao, C. Zhao, N. Tang, C. Song, Q. Li, W. Zhou, J. Jin, H. Haick, Y. Chen, D. Cui, *ACS Nano* **2022**, 16, 16584; e) A. R. Abbasi, K. Akhbari, A. Morsali, *Ultrason. Sonochem.* **2012**, 19, 846; f) Y. Zhang, X. Shen, P. Ma, Z. Peng, K. Cai, *Mater. Lett.* **2019**, 241, 18.
- [12] a) M. J. Duncan, P. S. Wheatley, E. M. Coghill, S. M. Vornholt, S. J. Warrender, I. L. Megson, R. E. Morris, *Mater. Adv.* **2020**, 1, 2509; b) Z. Yu, X. Li, X. Li, B. Zheng, D. Li, D. Xu, F. Wang, *Adv. Funct. Mater.* **2023**, 33, 2305995; c) N. Rabiee, M. Bagherzadeh, M. H. Haris, A. M. Ghadiri, F. M. Moghaddam, Y. Fatahi, R. Dinarvand, A. Jarahiyan, S. Ahmadi, M. Shokouhimehr, *ACS Appl. Mater. Interfaces* **2021**, 13, 10796; d) K. Huang, W. Liu, W. Wei, Y. Zhao, P. Zhuang, X. Wang, Y. Wang, Y. Hu, H. Dai, *ACS Nano* **2022**, 16, 19491; e) A. Arenas-Vivo,

- G. Amariei, S. Aguado, R. Rosal, P. Horcajada, *Acta Biomater.* **2019**, 97, 490; f) B. Claes, T. Boudewijns, L. Muchez, G. Hooyberghs, E. V. Van der Eycken, J. Vanderleyden, H. P. Steenackers, D. E. De Vos, *ACS Appl. Mater. Interfaces* **2017**, 9, 4440; g) M. Liu, L. Wang, X. Zheng, Z. Xie, *ACS Appl. Mater. Interfaces* **2017**, 9, 41512; h) M. Yu, D. You, J. Zhuang, S. Lin, L. Dong, S. Weng, B. Zhang, K. Cheng, W. Weng, H. Wang, *ACS Appl. Mater. Interfaces* **2017**, 9, 19698; i) J. Zhang, X. Ke, M. Huang, X. Pei, S. Gao, D. Wu, J. Chen, Y. Weng, *Biomater. Sci.* **2022**, 11, 322.
- [13] T. Kunisada, K. Yamada, S. Oda, O. Hara, *Dermatology* **1997**, 195, 14.
- [14] X. Han, G. Boix, M. Balcerzak, O. Hernando Moriones, M. Cano-Sarabia, P. Cortés, N. Bastús, V. Puentes, M. Llagostera, I. Imaz, D. Maspoch, *Adv. Funct. Mater.* **2022**, 32, 2112902.
- [15] a) W. Xi, V. Hegde, S. D. Zoller, H. Y. Park, C. M. Hart, T. Kondo, C. D. Hamad, Y. Hu, A. H. Loftin, D. O. Johansen, Z. Burke, S. Clarkson, C. Ishmael, K. Hori, Z. Mamouei, H. Okawa, I. Nishimura, N. M. Bernthal, T. Segura, *Nat. Commun.* **2021**, 12, 5473; b) Z. Huang, S. Nazifi, K. Cheng, A. Karim, H. Ghasemi, *Chem. Eng. J.* **2021**, 422, 130085.
- [16] a) Z. Xiu, M. Yang, R. Wu, C. Lei, H.-M. Ren, B. Yu, S. Gao, S. Duan, D. Wu, F.-J. Xu, *Chem. Eng. J.* **2023**, 451, 138495. b) Z. Zhang, L. Wang, J. Liu, H. Yu, X. Zhang, J. Yin, S. Luan, H. Shi, *Small* **2023**, 19, 2304379; c) F. J. Davis, G. R. Mitchell, in *Bio-Materials and Prototyping Applications in Medicine*, (Eds.: P. Bartolo, B. Bidanda), Springer, New York, NY, USA **2008**, pp. 27–48.
- [17] a) L. Pottié, *SOFW J.* **2019**, 145, 8. b) Hair Care Market Trends, Concepts and Solutions, <https://www.personal-care.basf.com/docs/default-source/press-center-files/personal-care-in-the-media/2020/h-pc-today-panel-discussion-hair-care-rambutan.pdf> (accessed: March 2019); c) Covestro Press / Beauty with responsibility, <https://www.covestro.com/press/beauty-with-responsibility/> (accessed: May 2024).
- [18] a) J. Troyano, C. Çamur, L. Garzón-Tovar, A. Carné-Sánchez, I. Imaz, D. Maspoch, *Acc. Chem. Res.* **2020**, 53, 1206; b) A. Carné-Sánchez, I. Imaz, M. Cano-Sarabia, D. Maspoch, *Nat. Chem.* **2013**, 5, 203; c) S. Wintzheimer, L. Luthardt, K. Le Anh Cao, I. Imaz, D. Maspoch, T. Ogi, A. Bück, D. P. Debecker, M. Faustini, K. Mandel, *Adv. Mater.* **2023**, 35, 2306648.
- [19] J. Yoo, Y.-Y. Won, *ACS Biomater. Sci. Eng.* **2020**, 6, 6053.
- [20] a) C. Aharoni, F. C. Tompkins, *Adv. Catal.* **1970**, 21, 1; b) V. F. D. Martins, C. V. Miguel, J. C. Gonçalves, A. E. Rodrigues, L. M. Madeira, *Chem. Eng. J.* **2022**, 434, 15.
- [21] a) I. Yeeling Wu, S. Bala, N. Škalko-Basnet, M. Pio di Cagno, *Eur. J. Pharm. Sci.* **2019**, 138, 105026; b) L. Wu, J. Li, Y. Wang, X. Zhao, Y. He, H. Mao, W. Tang, R. Liu, K. Luo, Z. Gu, *Adv. Mater.* **2023**, 35, 2305529; c) M. Fosca, J. V. Rau, V. Uskokovic, *Bioact. Mater.* **2022**, 7, 341.
- [22] A. F. Deyrieux, V. G. Wilson, *Cytotechnology* **2007**, 54, 77.
- [23] a) A. Perez-Gavilan, J. Vieira de Castro, A. Arana, S. Merino, A. Retolaza, S. A. Alves, A. Francone, N. Kehagias, C. M. Sotomayor-Torres, D. Cocina, R. Mortera, S. Crapanzano, C. J. Pelegrín, M. C. Garrigos, A. Jiménez, B. Galindo, M. C. Araque, D. Dykeman, N. M. Neves, J. M. Marimón, *Sci. Rep.* **2021**, 11, 6675; b) E. E. Mann, D. Manna, M. R. Mettetal, R. M. May, E. M. Dannemiller, K. K. Chung, A. B. Brennan, S. T. Reddy, *Antimicrob Resist Infect Control* **2014**, 3, 28.
- [24] X. Pan, N. Wu, S. Tian, J. Guo, C. Wang, Y. Sun, Z. Huang, F. Chen, Q. Wu, Y. Jing, Z. Yin, B. Zhao, X. Xiong, H. Liu, D. Zhou, *Adv. Funct. Mater.* **2022**, 32, 2112145.
- [25] J. R. Johnson, *Clin. Microbiol. Rev.* **1991**, 4, 80.
- [26] A. K. Pöntinen, J. Top, S. Arredondo-Alonso, G. Tonkin-Hill, A. R. Freitas, C. Novais, R. A. Gladstone, M. Pesonen, R. Meneses, H. Pesonen, J. A. Lees, D. Jamroz, S. D. Bentley, V. F. Lanza, C. Torres, L. Peixe, T. M. Coque, J. Parkhill, A. C. Schürch, R. J. L. Willems, J. Corander, *Nat. Commun.* **2021**, 12, 1523.
- [27] T. D. Trinh, E. J. Zasowski, K. C. Claeys, A. M. Lagnf, S. Kidambi, S. L. Davis, M. J. Rybak, *Diagn. Microbiol. Infect. Dis.* **2017**, 89, 61.
- [28] J.-F. Timsit, E. Ruppé, F. Barbier, A. Tabah, M. Bassetti, *Intensive Care Med* **2020**, 46, 266.
- [29] J. A. Vazquez, V. Sanchez, C. Dmuchowski, L. M. Dembry, J. D. Sobel, M. J. Zervos, *J. Infect. Dis.* **1993**, 168, 195.